

# A weak lensing estimate from GEMS of the virial to stellar mass ratio in massive galaxies to $z \sim 0.8$

Catherine Heymans,<sup>1,2\*</sup> Eric F. Bell,<sup>2</sup> Hans-Walter Rix,<sup>2</sup> Marco Barden,<sup>2</sup> Andrea Borch,<sup>2,3</sup> John A. R. Caldwell,<sup>4</sup> Daniel H. McIntosh,<sup>5</sup> Klaus Meisenheimer,<sup>2</sup> Chien Y. Peng,<sup>6</sup> Christian Wolf,<sup>7</sup> Steven V. W. Beckwith,<sup>6,8</sup> Boris Häußler,<sup>2</sup> Knud Jahnke,<sup>2</sup> Shardha Jogee,<sup>9</sup> Sebastian F. Sánchez,<sup>10</sup> Rachel Somerville<sup>2</sup> and Lutz Wisotzki<sup>11</sup>

<sup>1</sup>Department of Physics and Astronomy, University of British Columbia, 6224 Agricultural Road, Vancouver, V6T 1Z1, Canada

<sup>2</sup>Max-Planck-Institut für Astronomie, Königstuhl, D-69117, Heidelberg, Germany

<sup>3</sup>Astronomisches Rechen-Institut, Mönchhofstr. 12-14, D-69120 Heidelberg, Germany

<sup>4</sup>University of Texas, McDonald Observatory, Fort Davis, TX 79734, USA

<sup>5</sup>Department of Astronomy, University of Massachusetts, 710 North Pleasant Street, Amherst, MA 01003, USA

<sup>6</sup>Space Telescope Science Institute, 3700 San Martin Drive, Baltimore, MD 21218, USA

<sup>7</sup>Department of Astrophysics, Denys Wilkinson Building, University of Oxford, Keble Road, Oxford OX1 3RH

<sup>8</sup>Department of Physics & Astronomy, Johns Hopkins University, Baltimore, MD 21218, USA

<sup>9</sup>Department of Astronomy, University of Texas at Austin, 1 University Station, C1400 Austin, TX 78712-0259, USA

<sup>10</sup>Centro Hispano Aleman de Calar Alto, C/Jesus Durban Remon 2-2, E-04004 Almeria, Spain

<sup>11</sup>Astrophysikalisches Institut Potsdam, An der Sternwarte 16, 14482 Potsdam, Germany

Accepted 2006 June 19. Received 2006 June 2; in original form 2006 April 28

## ABSTRACT

We present constraints on the evolution of the virial to stellar mass ratio of galaxies with high stellar masses in the redshift range  $0.2 < z < 0.8$ , by comparing weak lensing measurements of virial mass  $M_{\text{vir}}$  with estimates of stellar mass  $M_{\text{star}}$ . For a complete sample of galaxies with  $\log(M_{\text{star}}/M_{\odot}) > 10.5$ , where the majority show an early-type morphology, we find that the virial mass to stellar mass ratio is given by  $M_{\text{vir}}/M_{\text{star}} = 53_{-16}^{+13}$ . Assuming a baryon fraction from the concordance cosmology, this corresponds to a stellar fraction of baryons in massive galaxies of  $\Omega_{\text{b}}^*/\Omega_{\text{b}} = 0.10 \pm 0.03$ . Analysing the galaxy sample in different redshift slices, we find little or no evolution in the virial to stellar mass ratio, and place an upper limit of  $\sim 2.5$  on the growth of massive galaxies through the conversion of gas into stars from  $z = 0.8$  to the present day.

**Key words:** gravitational lensing – galaxies: evolution – galaxies: general – galaxies: haloes – cosmology: observations.

## 1 INTRODUCTION

In the standard cold dark matter paradigm, luminous galaxies reside in massive dark matter haloes. The large-scale clustering and formation of these luminous galaxies are driven by the clustering and formation histories of their dark matter haloes. In contrast, the visible properties of such galaxies are a strong function of the complex physics of baryonic matter, in particular the laws governing stellar and active galactic nucleus feedback, gas cooling and star formation. The luminosities and colours of galaxies are a strong function of the efficiencies of these processes, and our inability to model them robustly is a critical limitation of current models of galaxy formation

and evolution (as discussed, for example, by Benson et al. 2003). A key way to constrain the efficiency of such processes is to measure empirically the ratio of the stellar mass to the total virial mass of the halo and galaxy system, for certain subsets of the galaxy population. Assuming a baryon to dark matter fraction from the concordant cosmology, it is then possible to determine empirically the fraction of baryons that manage to cool and condense into stars in haloes of a given mass. Such measurements of the mass out to  $\geq 100$  kpc scales not only constrain the efficiency of complex ‘gastrophysical’ processes, but also empirically calibrate and test halo occupation distribution analyses of galaxy properties (see, for example, Yang et al. 2005).

Satellite galaxies (Zaritsky & White 1994; Prada et al. 2003) and weak gravitational lensing (see the review by Bartelmann & Schneider 2001) are currently the most promising methods available

\*E-mail: heymans@physics.ubc.ca

to probe virial masses of dark matter haloes. In this Letter we focus on weak gravitational lensing, the weak distortion of distant sources by the gravitational field of foreground structure, as it provides a unique way to probe matter on all scales, at all redshifts, irrespective of its dynamical state or nature. Termed ‘galaxy–galaxy lensing’, the weak tangential shearing of background galaxies relative to foreground galaxies can therefore be used to probe the distribution of dark matter in galaxies, as first demonstrated by Brainerd, Blandford & Smail (1996).

In this Letter we combine information from two surveys of the *Chandra* Deep Field South: the ground-based COMBO-17 survey (Classifying Objects by Medium-Band Observations in 17 filters; Wolf et al. 2003) and the *Hubble Space Telescope* (*HST*) GEMS survey (Galaxy Evolution from Morphologies and Spectral energy distributions; Rix et al. 2004), in order to constrain the virial to stellar mass ratio in stellar massive galaxies out to  $z \sim 0.8$ . The 17-filter photometry of COMBO-17 provides accurate photometric redshifts with errors  $\sigma_z \sim 0.02(1+z)$ . COMBO-17 additionally provides stellar mass estimates  $M_{\text{star}}$  by fitting a parametrized star formation history to the low-resolution 17-band galaxy spectra (Borch et al. 2006), based on a Kroupa, Tout & Gilmore (1993) initial mass function (Kroupa IMF). The *HST* resolution of the GEMS imaging allows for high signal-to-noise ratio measurements of the ‘galaxy–galaxy’ lensing signal which can provide an ensemble estimate of the virial mass for (sub-)sets of galaxies. A detailed description of the galaxy–galaxy lensing analysis of GEMS and the resulting constraints on different dark matter halo profiles for different galaxy types will be presented in a forthcoming paper (Heymans et al., in preparation). For the purposes of this Letter, however, we focus on a complete sample of 626 lens galaxies with high stellar masses. We measure the virial to stellar mass ratio as a function of galaxy redshift to  $z \sim 0.8$ , presenting the first redshift-dependent galaxy–galaxy lensing analysis to be performed consistently over such a large redshift range.

This Letter is organized as follows. In Section 2 we describe the theory that underpins our measurement of virial masses and review the particulars of our analysis. We refer the reader to section 3 of Heymans et al. (2005, hereafter H05) for a lensing-specific description of the GEMS observations and the data reduction. In Section 3 we present constraints on the virial radius and the virial to stellar mass ratio for our full stellar massive galaxy sample, and convert the mass ratio into a stellar fraction of baryons. We compare our results with the low-redshift results of Hoekstra et al. (2005, hereafter HHYLG) and Mandelbaum et al. (2006, hereafter M06), and investigate the dependence of the virial to stellar mass ratio on galaxy redshift, setting constraints on the growth of massive galaxies through the conversion of gas into stars from  $z \sim 0.8$  to the present day. We discuss the implications of these results and conclude in Section 4. Throughout this Letter we assume a  $\Lambda$  cold dark matter ( $\Lambda$  CDM) cosmology with  $\Omega_m = 0.3$ ,  $\Omega_\Lambda = 0.7$  and  $H_0 = 100 h \text{ km s}^{-1} \text{ Mpc}^{-1}$ . For our virial to stellar mass ratio measurement we set  $h = 0.7$ .

## 2 MEASURING VIRIAL MASSES WITH GALAXY–GALAXY LENSING

The mass of a foreground ‘lens’ galaxy will weakly shear the images of background or ‘source’ galaxies. The extent of this tangential shearing as a function of lens and source position can be directly derived from the density distribution of the lens galaxy. In this Letter we adopt the Navarro, Frenk & White (1997, hereafter NFW) (e.g. Navarro, Frenk & White 1997) profile as a model for dark matter haloes, where the density distribution of a halo at redshift  $z$  is

given by

$$\rho(r) = \frac{\delta_c \rho_c(z)}{(r/r_s)(1+r/r_s)^2}. \quad (1)$$

$\delta_c$  is the characteristic density,  $r_s$  is the scale radius and  $\rho_c(z)$  is the critical density<sup>1</sup> given by  $3H(z)^2/8\pi G$ . The virial radius  $r_\Delta$  is defined as the radius where the mass density of the halo is equal to  $\Delta \times \rho_c$ . Eke et al. (1996) show that for a flat  $\Lambda$  cosmology, assuming a spherical collapse model,

$$\Delta(\Omega_m, \Lambda) = 178\Omega_m^{0.45}. \quad (2)$$

For the cosmology adopted here,  $\Delta \approx 100$  at  $z = 0$ , and  $\Delta \approx 150$  at  $z = 0.8$ . The corresponding virial mass<sup>2</sup>  $M_\Delta$  is given by

$$M_\Delta = \Delta \rho_c \frac{4\pi}{3} r_\Delta^3. \quad (3)$$

Defining the concentration parameter as  $c = r_\Delta/r_s$ , the characteristic halo density  $\delta_c$  is then given by

$$\delta_c = \frac{\Delta}{3} \frac{c^3}{\ln(1+c) - c/(1+c)}. \quad (4)$$

Note that for a given CDM cosmology, halo mass  $M_{\text{vir}}$  and concentration  $c$ , or scale radius  $r_s$ , are related (Navarro et al. 1997; Bullock et al. 2001; Eke, Navarro & Steinmetz 2001), where the dependence is calculated through fits to numerical simulations.

The expression for the weak lensing shear  $\gamma$  induced by an NFW dark matter halo is given in Wright & Brainerd (2000).

### 2.1 Lens galaxy sample selection

To measure accurate virial masses it is important to have accurate photometric redshifts. To compare virial mass with stellar mass we also require good stellar mass estimates. We therefore limit ourselves to a sample of lens galaxies with a measured COMBO-17 photometric redshift (this implies a magnitude limit of  $R < 24$ ) in the range  $0.2 < z < 0.8$ . For the purposes of this Letter we wished to create a complete sample of galaxies in order to be able to study the virial to stellar mass ratio as a function of redshift without the inclusion of potentially biasing selection effects. This requirement imposed a high stellar mass cut where  $\log(M_{\text{star}}/M_\odot) > 10.5$ , above which it has been shown that the COMBO-17 catalogue is complete in both redshift estimates and flux (Wolf et al. 2004; Borch et al. 2006). The Sérsic fits of these galaxies (see Barden et al. 2005; McIntosh et al. 2005) indicate that the majority of the lens sample ( $\sim 75$  per cent) are early-type galaxies with  $n > 2.5$ . Note that including an  $n > 2.5$  Sérsic selection criterion such that our lens sample contains only early-type galaxies does not change our results except for decreasing the lensing signal-to-noise ratio. The galaxy sample has an average photometric redshift accuracy of  $\delta_z \sim 0.03$  and a mean stellar mass of  $\langle M_{\text{star}} \rangle = 7.2 \times 10^{10} M_\odot$ . The galaxies are very luminous with a mean Sloan Digital Sky Survey (SDSS)  $r$ -band luminosity  $\langle L \rangle = 2.4 L_*$ , where  $L_* = 10^{10} h^{-2} L_\odot$ . They also have a low dynamic range of galaxy luminosity with  $\sigma(\log L/L_*) = 0.2$ .

<sup>1</sup>Note that within the galaxy–galaxy lensing literature  $\rho_c$  is often defined differently. In this Letter we follow the definition given in the appendix of Navarro et al. (1997).

<sup>2</sup>This definition of virial mass is directly equivalent to that used by HHYLG as  $\Delta(z) \rho_c(z) = \Delta_{\text{vir}}(z) \rho_{\text{bg}}(z)$ , where  $\Delta_{\text{vir}}$  and  $\rho_{\text{bg}}$  are given after equation (9) of HHYLG.

Source galaxies with which to measure the galaxy–galaxy lensing signal are selected from the GEMS data as described in section 4.3 of H05. This yields a number density of 65 source galaxies per square arcminute.

The lens redshift limits were chosen to optimize the measured signal. Galaxies at higher redshifts typically have poorer photometric redshift accuracy, and they also provide rather weak constraints owing to the reduced number of background sources. The lower redshift limit results from the fact that we exclude all sources for which lenses might lie outwith the GEMS area. For a given maximum impact parameter  $r_{\max}$ , this corresponds to a minimum angular separation  $\theta(z_{\min})$  from the edge of the field. We therefore include the lower redshift limit to reduce  $\theta(z_{\min})$ , thus including as many sources as possible.

In this Letter we will make two assumptions. As our lens sample spans a low dynamic range in luminosities, we will assume that the halo virial radius  $r_{\Delta}$  of our lens sample is constant. M06 find that stellar mass is a good galaxy-type-dependent proxy for halo mass. We will therefore also assume that, on average, the halo virial mass of our galaxy sample scales linearly with galaxy stellar mass by defining the following scaling relation:

$$M_{\text{vir}} = k_{\text{NFW}} M_{\text{star}}. \quad (5)$$

Using the mass/concentration relations from Navarro et al. (1997), the halo profile of a galaxy in our sample can then be uniquely described by an NFW model with one free parameter: either  $r_{\Delta}$  or  $k_{\text{NFW}}$ .

## 2.2 Analysis method

We use the method of Kaiser, Squires & Broadhurst (1995), Lupino & Kaiser (1997) and Hoekstra et al. (1998) (KSB+) to obtain an estimate of the observed ellipticity  $\epsilon^{\text{obs}}$  of each source galaxy in the GEMS survey. In the weak shear limit, where  $\gamma \ll 1$ , the observed ellipticity  $\epsilon^{\text{obs}} \approx \epsilon^{\text{s}} + \gamma$ , where  $\epsilon^{\text{s}}$  is the intrinsic source galaxy ellipticity. The application of the method to the GEMS data set is described in detail in H05 along with the results of several diagnostic tests which confirm the success of this method at removing point spread function distortions. The level of shear calibration bias expected with the H05 implementation of KSB+ has been shown to be  $\sim 3$  per cent (Heymans et al. 2006) which is well within the statistical uncertainties of this analysis.

In order to interpret the measured average tangential shear in the context of NFW halo lensing, redshift information for both the lens and source galaxies is required (see for example Kleinheinrich et al. 2005). The COMBO-17 survey provides accurate photometric redshifts for the foreground lens sample of galaxies with  $R < 24$  (Wolf et al. 2004). For the fainter source galaxy sample only the redshift probability distribution is known (see section 6 of H05). The maximum likelihood method of Schneider & Rix (1997) was designed to take advantage of such a data set by analysing the galaxy–galaxy lensed shear statistically, and it is this method that we use in the following analysis and describe below.

For a model galaxy density profile, in the case where all galaxy redshifts are known, the weak shear  $\gamma$  experienced by each source galaxy can be predicted by summing up the shear contributions from all the foreground lens galaxies, taking into account the multiple weak deflections that a source may experience (Brainerd 2005). Note that when a sample of lenses are selected from the foreground galaxy population, the other foreground galaxies act as a source of noise without introducing bias (Kleinheinrich et al. 2006). In this analysis the redshifts of the source galaxies are unknown, and we therefore

assign those galaxies a magnitude-dependent redshift probability distribution  $p(z, \text{mag})$  [(15) in H05] and calculate the expectation value of the shear  $\langle \gamma \rangle$ . This is done through Monte Carlo integration, drawing a source galaxy redshift estimate  $z_{\text{s}}^{\nu}$  from the distribution  $p(z, \text{mag})$ ,  $\nu = 1 \dots N_{\text{MC}}$  times, where  $N_{\text{MC}} = 100$  in this analysis. For each  $z_{\text{s}}^{\nu}$  estimate the induced galaxy–galaxy lensing shear  $\gamma^{\nu}$  is calculated with the resulting mean shear given by

$$\langle \gamma \rangle = \frac{1}{N_{\text{MC}}} \sum_{\nu=1}^{N_{\text{MC}}} \gamma^{\nu}. \quad (6)$$

Note that in practice we only consider the shear from those lenses where the angular separation from the source  $\theta < r_{\max}/D_1$  with  $r_{\max} = 300 h^{-1}$  kpc. The intrinsic source galaxy ellipticity  $\epsilon^{\text{s}}$  is then calculated,  $\epsilon^{\text{s}} \approx \epsilon^{\text{obs}} - \gamma$ . The distribution of each component of the observed galaxy ellipticity is well described, for the GEMS survey, by a Gaussian of width  $\sigma_{\epsilon} = 0.31$ . As the induced shear  $\gamma$  is weak, the probability for observing an intrinsic ellipticity of  $\epsilon^{\text{s}}$  is then given by

$$P(\epsilon^{\text{s}}) = \frac{1}{2\pi\sigma_{\epsilon}^2} \exp\left(-\frac{|\epsilon^{\text{s}}|^2}{2\sigma_{\epsilon}^2}\right). \quad (7)$$

The best-fitting dark matter halo parameters are determined by maximizing the likelihood  $L = \Pi [P(\epsilon^{\text{s}})_i]$  where the product extends over all source galaxies  $i$ .

## 3 RESULTS

In this section we present our constraints on the virial radius and the virial to stellar mass ratio of the stellar massive galaxies in our lens sample. Assuming that the chosen subset of lens galaxies have a constant virial radius, we find  $r_{\Delta} = 204^{+18}_{-22} h^{-1}$  kpc. This corresponds to a virial mass of  $M_{\text{vir}} = 29.8^{+7.9}_{-9.6} \times 10^{11} h^{-1} M_{\odot}$  for a galaxy at  $z \sim 0.65$ , the median redshift of the lens sample. Note that the corresponding virial mass is dependent on the redshift of the halo because of the redshift dependence of the critical density  $\rho_c$  and  $\Delta$  (equation 3). For our mean galaxy luminosity we find an average mass-to-light ratio for the stellar massive galaxies of  $M_{\text{vir}}/L = 123 \pm 36 h M_{\odot}/L_{\odot}$ . To illustrate this result, obtained using the maximum likelihood method described in Section 2.2, Fig. 1 shows the average tangential alignment  $\langle \gamma_{\text{t}} \rangle$  of source galaxies with respect to the lens sample as a function of angular separation on the sky. The measured signal  $\langle \gamma_{\text{t}} \rangle$  is well fitted by the expected signal around an NFW halo at the median redshift of the lens sample with

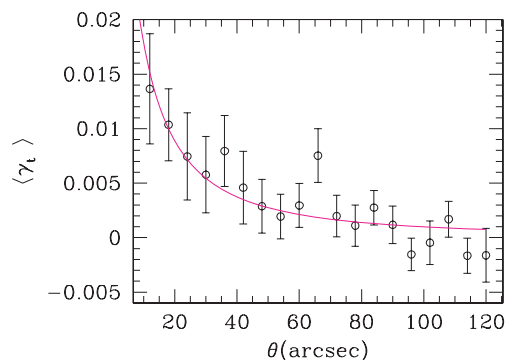


**Figure 1.** The average tangential alignment  $\langle \gamma_{\text{t}} \rangle$  of source galaxies with respect to the lens sample as a function of angular separation on the sky  $\theta$ . The solid curve shows the theoretical lensing signal from an NFW halo at  $z = 0.65$ , the median redshift of the lens sample, with the maximum likelihood method constrained virial radius  $r_{\Delta} = 204 h^{-1}$  kpc.

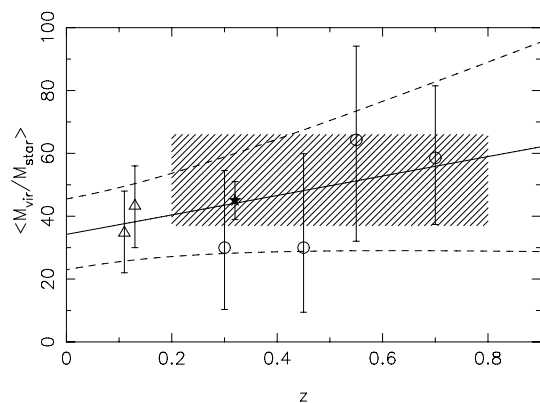


**Figure 2.** The virial mass to stellar mass ratio as a function of galaxy redshift (circles). The result at  $z = 0.32$  is from HHYLG (star). The results at  $z = 0.11$  and  $z = 0.13$  are from M06 (triangles) measured from different stellar mass selected samples that best match our lens sample. The errors are  $1\sigma$  in all cases, with the exception being M06 who quote  $3\sigma$  errors. The hatched region is the  $1\sigma$  confidence region for the virial mass to stellar mass ratio measured from GEMS over the full redshift range  $0.2 < z < 0.8$ . The solid line indicates the best linear fit to  $M_{\text{vir}}/M_{\text{star}}(z)$  and the dashed lines denote the  $1\sigma$  errors to this fit.

the maximum likelihood method constrained virial radius of  $r_{\Delta} = 204 h^{-1}$  kpc.

Our results are in good agreement with the results of HHYLG, who find  $M_{\text{vir}} = 23.3^{+5.6}_{-5.1} \times 10^{11} h^{-1} M_{\odot}$  for their luminous galaxy sample at  $z \sim 0.32$ , where  $\langle L \rangle = 2.49 L_{*}$ . Scaling our results to  $z = 0.32$  we find  $M_{\text{vir}} = 17.8^{+4.7}_{-5.7} \times 10^{11} h^{-1} M_{\odot}$ . These results are also in good agreement with the results of M06, who find a virial mass for central galaxies (as opposed to satellite galaxies) of  $M_{\text{cent}} = 14.1^{+5.6}_{-5.3} \times 10^{11} h^{-1} M_{\odot}$ , for a sample of early-type galaxies with mean stellar mass  $\langle M_{\text{star}} \rangle = 5.8 \times 10^{10} M_{\odot}$  and mean luminosity  $\langle L \rangle \sim 1.3 L_{*}$ . This galaxy sample has a mean redshift  $z \sim 0.11$ , and scaling our results to this redshift we find a consistent virial mass of  $M_{\text{vir}} = 12.5^{+3.3}_{-4.0} \times 10^{11} h^{-1} M_{\odot}$  for our sample of stellar massive galaxies with mean stellar mass  $\langle M_{\text{star}} \rangle = 7.2 \times 10^{10} M_{\odot}$  and mean luminosity  $\langle L \rangle \sim 2.4 L_{*}$ .

In Section 2.1 we introduced a stellar mass scaling to relate halo mass to stellar mass, which we choose to be linear.<sup>3</sup> For the full lens sample we measure a best-fitting value for the NFW virial mass to stellar mass ratio as  $k_{\text{NFW}} = 53^{+13}_{-16}$  with  $1\sigma$  errors. Note that  $k_{\text{NFW}} = 1$  is ruled out with 99.99 per cent confidence. Our result is in good agreement with the results of HHYLG and M06, as shown in Fig. 2. HHYLG find  $k_{\text{NFW}} = 45 \pm 6$  for a scaled Salpeter IMF which is similar to the Kroupa IMF used in this analysis.<sup>4</sup> M06 find  $k_{\text{NFW}} = 35 \pm 13$  using a Kroupa IMF, for the sample of early-type galaxies whose average stellar mass best matches the average stellar mass of our sample, as discussed above. For a higher stellar mass selected sample with  $\langle M_{\text{star}} \rangle = 11.2 \times 10^{10} M_{\odot}$ , M06 find  $k_{\text{NFW}} = 43 \pm 13$ . As  $\sim 20$  per cent of our sample would fall into this mass bin, we also show this result in Fig. 2.

Following the analysis of HHYLG and M06 we convert our virial to stellar mass ratio into a stellar baryon fraction  $f_{*}$  by assuming

<sup>3</sup>Note that we also tested non-linear stellar mass scaling, but found for our complete sample of  $\log(M_{\text{star}}/M_{\odot}) > 10.5$  galaxies that any non-linear component was consistent with zero within the noise.

<sup>4</sup>Note that the Kroupa IMF and scaled Salpeter IMF are roughly half the mass of a Salpeter IMF and hence our results would scale to  $k_{\text{NFW}}^{\text{S}} \sim 27$  in comparison to the HHYLG Salpeter IMF measurement of  $k_{\text{NFW}}^{\text{S}} = 26 \pm 4$ .

that the baryon to dark matter ratio in massive galaxies is given by the global value  $\Omega_{\text{b}}/\Omega_{\text{m}} = 0.176 \pm 0.013$  (Spergel et al. 2006) such that

$$f_{*} = \frac{M_{\text{star}}}{M_{\text{vir}}} \frac{\Omega_{\text{m}}}{\Omega_{\text{b}}} \sim \Omega_{\text{b}}^{*}/\Omega_{\text{b}}. \quad (8)$$

The measured virial to stellar mass ratio then gives us a stellar baryon fraction of  $f_{*} = \Omega_{\text{b}}^{*}/\Omega_{\text{b}} = 0.10 \pm 0.03$ , suggesting that galaxies with high stellar masses are rather inefficient at converting baryons into stellar mass: only 10 per cent of the baryons are contained in stars. This result is in good agreement with the cosmic baryon budget of Fukugita, Hogan & Peebles (1998) who estimate the the amount of baryons in different states, finding the fraction of baryons in spheroids to be  $f_{*} \sim 0.12$ .

### 3.1 Redshift dependence

Splitting our galaxy sample into four redshift slices we show, in Fig. 2, that the virial to stellar mass ratio remains fairly constant as a function of galaxy redshift. For a linear fit to these results, together with the estimates of HHYLG and M06, we can constrain  $k_{\text{NFW}}(z) = (34 \pm 11) + (31 \pm 35)z$ . Comparing the virial to stellar mass ratio at  $z = 0$  and  $0.8$ , we find a  $1\sigma$  confidence region where  $0.8 < [k(z = 0.8)/k(z = 0)] < 2.6$ . The data therefore indicate that the virial to stellar mass ratio has evolved by a factor of  $\lesssim 2.5$  since  $z = 0.8$ .

## 4 DISCUSSION AND CONCLUSION

In this Letter, we use a weak gravitational lensing study of the *HST* GEMS survey, in combination with the 17-colour photometry of the COMBO-17 survey, to determine the ratio between virial and stellar mass in a complete sample of massive galaxies out to  $z \sim 0.8$ . We find a mean virial to stellar mass ratio  $M_{\text{vir}}/M_{\text{star}} = 53^{+13}_{-16}$  with little or no redshift evolution in this stellar mass fraction.

This result provides a high-redshift extension to the analysis of Hoekstra et al. (2005, HHYLG) and Mandelbaum et al. (2006, M06). The excellent agreement found between the results of this analysis, HHYLG and M06 is important to comment upon as the analyses were performed using very different techniques and came from very different surveys: HHYLG used the Red sequence Cluster Survey, a medium-deep 45.5 square degree ground-based survey in *BVRz*, while M06 used the shallow Sloan Digital all Sky Survey which is ground-based in *ugriz*. This analysis uses GEMS, a deep 0.25 square degree space-based survey with accompanying 17-band COMBO-17 data.

In this analysis we use stellar masses calculated from the best-fitting models of star formation history to the low-resolution 17-band galaxy spectra. M06 used a similar technique (Kauffmann et al. 2003). HHYLG used the simple relationship of Bell & de Jong (2001) that relates stellar mass to *B - V* colour. This relationship has a systematic uncertainty that is often estimated to be  $\sim 30$  per cent (Bell et al. 2003). Stellar mass uncertainty is indeed hard to avoid with all methods, however, owing to the unknown frequency of bursts of star formation and uncertainty in dust models (Borch et al. 2006). The fact all three results are in such close agreement, however, demonstrates that the simple models of HHYLG are consistent with the more complex star formation history models of COMBO-17 and M06, which bodes well for similar studies in future broad-band surveys.

We have applied the Schneider & Rix (1997) maximum likelihood method to set constraints on the virial radius and the virial to

stellar mass ratio using an NFW dark matter profile. This method takes into account the uncertainty in the redshift of both the source and lens galaxies, using a Monte Carlo technique, and includes the effects of the multiple deflection of light by successive foreground lens galaxies. In contrast, HHYLG measured the tangential shear around foreground galaxies for different luminosity bins and fitted this result with the shear expected from an NFW profile. The HHYLG galaxies were selected to be isolated such that the lensed background galaxies experience only the gravitational potential of the isolated galaxy. Their larger photometric redshift errors are more likely to scatter faint galaxies into higher luminosity bins than scatter bright galaxies into lower luminosity bins. This then leads to a bias in the measurement of the mass at fixed luminosity to a lower value. HHYLG therefore need to apply a correction factor to the virial masses which they determined from an analysis of mock catalogues. This bias is not a problem for our analysis owing to the higher accuracy of photometric redshifts and the use of the Schneider & Rix (1997) method. Our observational systematic errors are therefore minimal, and we are limited by random errors from smaller number statistics. The third analysis method of M06 used the halo model to extract information from the galaxy–galaxy lensing signal and separate contributions from central and satellite galaxies (Mandelbaum et al. 2005). The fact that these three very different methods produce consistent results serves as a good indication that the three results are robust.

This analysis is the first time that a comparison of the properties of luminous galaxies and their parent dark matter haloes has been performed consistently across a substantial span of cosmic time. The galaxy sample has been selected to be complete out to  $z \sim 0.8$  and we are therefore not subject to redshift-dependent selection biases. We have shown that for this galaxy sample, the majority of which show early-type morphologies, the virial to stellar mass ratio as a function of galaxy redshift remains fairly constant with  $M_{\text{vir}}/M_{\text{star}} \sim 50$ : specifically, we place a  $1\sigma$  upper limit on the growth of the stellar to virial mass ratio since  $z = 0.8$ , of a factor of  $< 2.6$ . Because we probe the ratio of stellar to virial mass, we cannot probe merger-driven growth of galaxies as stellar masses and virial masses grow in lock-step. Instead, our constraint effectively limits the conversion of gas into stars in the massive galaxy population, i.e. star formation, as a function of redshift. We therefore can conclude that the growth of stellar mass due to star formation is limited, to a factor of  $\lesssim 2.5$  from  $z = 0.8$  to the present day.

## ACKNOWLEDGMENTS

We thank Julio Navarro for making the NFW CHARDEN and ENS codes publicly available. We also thank Martina Kleinheinrich for useful discussions and the referee for his/her helpful comments. CH is supported by a CITA National Fellowship, and, with H-WR, acknowledges financial support from GIF. EFB is supported by the DFG's Emmy Noether Programme, CW by PPARC, CYP by STScI, and

SJ and DHM by NASA under LTSA Grant NAG5-13063 (SJ) and NAG5-13102 (DHM). Support for GEMS was provided by NASA through GO-9500 from STScI operated by AURA under NAS5-26555.

## REFERENCES

- Barden M. et al., 2005, *ApJ*, 635, 959  
 Bartelmann M., Schneider P., 2001, *Phys. Rep.*, 340, 291  
 Bell E. F., de Jong R. S., 2001, *ApJ*, 550, 212  
 Bell E. F., McIntosh D. H., Katz N., Weinberg M. D., 2003, *ApJS*, 149, 289  
 Benson A. J., Bower R. G., Frenk C. S., Lacey C. G., Baugh C. M., Cole S., 2003, *ApJ*, 599, 38  
 Borch A., Meisenheimer K., Bell E., Rix H. W., Wolf C., Dye S., Kleinheinrich M., Kovacs Z., Wisotzki L., 2006, *A&A*, 453, 869  
 Brainerd T. G., 2005, in Mellier Y., Meylan G., eds, *Proc. IAU Symp.* 225, *The Effects of Multiple Weak Deflections in Galaxy–Galaxy Lensing*. Cambridge University Press, Cambridge, p. 255  
 Brainerd T. G., Blandford R. D., Smail I., 1996, *ApJ*, 466, 623  
 Bullock J. S., Kolatt T. S., Sigad Y., Somerville R. S., Kravtsov A. V., Klypin A. A., Primack J. R., Dekel A., 2001, *MNRAS*, 321, 559  
 Eke V. R., Cole S., Frenk C. S., Navarro J. F., 1996, *MNRAS*, 281, 703  
 Eke V. R., Navarro J. F., Steinmetz M., 2001, *ApJ*, 554, 114  
 Fukugita M., Hogan C. J., Peebles P. J. E., 1998, *ApJ*, 503, 518  
 Heymans C. et al., 2005, *MNRAS*, 361, 160 (H05)  
 Heymans C. et al., 2006, *MNRAS*, 368, 1323  
 Hoekstra H., Franx M., Kuijken K., Squires G., 1998, *ApJ*, 504, 636  
 Hoekstra H., Hsieh B. C., Yee H. K. C., Lin H., Gladders M. D., 2005, *ApJ*, 635, 73 (HHYLG)  
 Kaiser N., Squires G., Broadhurst T., 1995, *ApJ*, 449, 460  
 Kauffmann G. et al., 2003, *MNRAS*, 341, 33  
 Kleinheinrich M. et al., 2005, *A&A*, 439, 513  
 Kleinheinrich M. et al., 2006, *A&A*, in press (astro-ph/0412615)  
 Kroupa P., Tout C. A., Gilmore G., 1993, *MNRAS*, 262, 545  
 Luppino G. A., Kaiser N., 1997, *ApJ*, 475, 20  
 McIntosh D. H. et al., 2005, *ApJ*, 632, 191  
 Mandelbaum R., Tasitsiomi A., Seljak U., Kravtsov A. V., Wechsler R. H., 2005, *MNRAS*, 362, 1451  
 Mandelbaum R., Seljak U., Kauffmann G., Hirata C. M., Brinkmann J., 2006, *MNRAS*, 368, 715 (M06)  
 Navarro J. F., Frenk C. S., White S. D. M., 1997, *ApJ*, 490, 493  
 Prada F. et al., 2003, *ApJ*, 598, 260  
 Rix H.-W. et al., 2004, *ApJS*, 152, 163  
 Schneider P., Rix H., 1997, *ApJ*, 474, 25  
 Spergel D. et al., 2006, *ApJ*, submitted (astro-ph/0603449)  
 Wolf C. et al., 2004, *A&A*, 421, 913  
 Wolf C., Meisenheimer K., Rix H.-W., Borch A., Dye S., Kleinheinrich M., 2003, *A&A*, 401, 73  
 Wright C. O., Brainerd T. G., 2000, *ApJ*, 534, 34  
 Yang X., Mo H. J., Jing Y. P., van den Bosch F. C., 2005, *MNRAS*, 358, 217  
 Zaritsky D., White S. D. M., 1994, *ApJ*, 435, 599

This paper has been typeset from a  $\text{\TeX}/\text{\LaTeX}$  file prepared by the author.